

# Effect of horizontal grid resolution on the near-equilibrium solution of a global ocean–sea ice model

P. B. Duffy

Climate System Modeling Group, Lawrence Livermore National Laboratory, Livermore, California, USA

M. E. Wickett

Center for Applied Scientific Computing, Lawrence Livermore National Laboratory, Livermore, California, USA

K. Caldeira

Climate System Modeling Group, Lawrence Livermore National Laboratory, Livermore, California, USA

Received 26 September 2000; revised 16 July 2001; accepted 17 July 2001; published 18 July 2002.

[1] We compare the near-equilibrium solution of a global ocean/sea ice model at a horizontal grid resolution of  $1^\circ \times 1^\circ$  to near-equilibrium solutions obtained in two configurations at  $4^\circ$  (longitude)  $\times$   $2^\circ$  (latitude) resolution. All simulations use realistic, smoothed topography and monthly averaged climatological forcings. Our comparison of the results emphasizes large-scale features relevant to global climate change. Since neither the  $1^\circ \times 1^\circ$  simulation nor the  $4^\circ \times 2^\circ$  simulations resolves ocean eddies, our results do not address the possible importance of resolving eddies in ocean-climate simulations. There are significant differences between the  $1^\circ \times 1^\circ$  and  $4^\circ \times 2^\circ$  simulations, most notably in the Arctic Ocean. However, the large-scale features of the model solutions are very similar at the two resolutions and in many cases are more sensitive to a large difference in horizontal viscosity than to the difference in resolution. This suggests that other approaches to improving the solution of ocean-climate models will be more effective than increases in horizontal resolution outside the eddy-resolving regime. **INDEX TERMS:** 1620 Global Change: Climate dynamics (3309); 1635 Global Change: Oceans (4203); 3210 Mathematical Geophysics: Modeling; 4532 Oceanography: Physical: General circulation; **KEYWORDS:** ocean model, resolution, sea ice model, equilibrium solution

## 1. Introduction

[2] Because of the roughly 1000 year characteristic time-scale for vertical overturning in the ocean, simulations of the ocean circulation require thousands of simulated years to approach equilibrium (i.e., for the solution to adjust to stationary boundary conditions). Simulations that include the ocean carbon cycle typically equilibrate even more slowly, requiring tens of thousand of years to reach near-equilibrium. The reasons for this are the multithousand year timescales associated with carbonate dissolution and with the radioactive decay of  $^{14}\text{C}$ . Because of limited computer resources, multimillennial simulations using global eddy-resolving ocean models are not possible at present and are not anticipated in the near future. Thus, for simulations of climate change, especially those treating the ocean carbon cycle, there is a continuing need for coarse (non-eddy-resolving) global ocean model simulations. Despite this it is unclear to what extent finer resolution improves the results of ocean models outside the eddy-resolving regime. That is the question addressed by this paper.

[3] The need for higher grid resolution in climate models is often discussed [e.g., *McAvaney et al.*, 2001]. Despite this,

relatively few studies have been published that systematically examine the effect of grid resolution on aspects of ocean model solutions that are relevant to climate simulation. Other resolution studies, for example, *McClean et al.* [1997] and *Bryan and Smith* [1998], have compared simulated mesoscale variability in simulations at several eddy-resolving resolutions to TOPEX/Poseidon and similar data. *Washington et al.* [1994] compared results of 100 year simulations of the Semtner-Chervin model [*Semtner and Chervin*, 1988, 1992] at three different resolutions:  $5^\circ \times 5^\circ$  with 4 levels in the vertical and  $1^\circ \times 1^\circ$  and  $0.5^\circ \times 0.5^\circ$  with 20 levels in the vertical. *Covey* [1995] looked at the effect of grid resolution on circulation and latitudinal heat transport in several short simulations of the Semtner-Chervin model [*Semtner and Chervin*, 1988, 1992]. The horizontal resolutions examined by Covey range from very coarse ( $4^\circ \times 4^\circ$ ) to one that begins to resolve eddies ( $0.25^\circ \times 0.25^\circ$ ). *Fanning and Weaver* [1997] looked at heat transport by the atmosphere and ocean in a coupled model consisting of an energy/moisture balance atmospheric model, coupled to a version of the Geophysical Fluid Dynamics Laboratory (GFDL) ocean model configured with resolutions ranging from  $1/4^\circ \times 1/4^\circ$  to  $4^\circ \times 4^\circ$ . *Gent et al.* [1998] compared solutions of the National Center for Atmospheric Research (NCAR) Ocean Model at roughly  $2^\circ \times 2^\circ$  and roughly  $3^\circ \times 3^\circ$  and found relatively small differences.

**Table 1.** Salient Features of the Simulations Described Here<sup>a</sup>

Simulation	Horizontal Viscosity Coefficient, $\text{cm}^2 \text{s}^{-1}$	Isopycnal Diffusion, $\text{cm}^2 \text{s}^{-1}$	Thickness Diffusion, $\text{cm}^2 \text{s}^{-1}$	High-Latitude Filtering?	Tracer $\Delta t$ , s	Momentum $\Delta t$ , s	Relative Computational Cost
1 $\times$ 1	$10^8$	$2 \times 10^7$	$1 \times 10^7$	Yes	21,600	360	32
4 $\times$ 2 HV	$10^9$	$2 \times 10^7$	$1 \times 10^7$	Yes	86,400	1440	1
4 $\times$ 2 LV	$10^8$	$2 \times 10^7$	$1 \times 10^7$	Yes	86,400	1440	1
4 $\times$ 2 NF	$10^8$	$2 \times 10^7$	$1 \times 10^7$	No	14,400	240	6

<sup>a</sup>Column 1 identifies the simulation. Column 2 lists a viscosity coefficient, which is used in (1) to yield horizontal viscosities.

[4] Here we compare the results of a near-equilibrium simulation at  $1^\circ \times 1^\circ$  to those of several simulations at  $4^\circ$  (longitude)  $\times$   $2^\circ$  (latitude). This study differs from previous work in several respects. First, we are examining effects of horizontal grid resolution on near-equilibrium model solutions; that is, we have run the model long enough that the effect of initial conditions on the solution is small. (It is worth noting that our  $1^\circ \times 1^\circ$  simulation is the finest-resolution near-equilibrium global ocean simulation we know of.) Second, we are using a coupled ocean-sea ice model, whereas previous work used either ocean-only models, or (in the case of *Fanning and Weaver* [1997]) an ocean-sea ice model coupled to a simplified representation of the atmosphere. Third, our model is purely prognostic, whereas *Covey* [1995] used “robust diagnostic forcing” (nudging of simulated temperatures and salinities toward observed values below the surface). Fourth, all the solutions we are comparing were obtained at resolutions that do not come close to resolving mesoscale eddies. Thus our results shed light not on the possible importance of resolving eddies but rather on the possible importance of better resolution of the physics, topography, and forcing within the non-eddy-resolving domain. Finally, we look at many aspects of the model’s solutions, whereas at least some previous studies have focused exclusively on latitudinal heat transport. It should be pointed out that we have looked at sensitivity of the time-averaged solution, but not of the variability of the solution, to model resolution. In addition, in our study the solutions are strongly constrained by surface boundary conditions; thus a coupled ocean-atmosphere model might display stronger sensitivity to ocean model resolution.

[5] The outline of the remainder of the paper is as follows. In section 2 we describe the model used here and the simulations we have performed. In section 3 we present our results. In section 4 we give conclusions.

## 2. Model Description

[6] The simulations discussed here were all performed with the Lawrence Livermore National Laboratory (LLNL) ocean–sea ice model. This model is based on version 1.0 of the GFDL ocean model. Enhancements include the addition of the Gent-McWilliams eddy parameterization [*Gent and McWilliams*, 1990], coupling to a parallel version of the Oberhuber sea ice model [*Oberhuber*, 1993], and replacement of the “rigid lid” approximation with a “free-surface” approach to solving for barotropic velocities [*Killworth et al.*, 1991]. The LLNL model is described in more detail by *Duffy and Caldeira* [1997] and by *Wickett et al.* [2000].

[7] All simulations described here use a global domain. Topography is essentially realistic but has been lightly smoothed to minimize numerical problems and to assure that topographic changes generally occur on a scale larger than the model grid. All surface forcings are obtained by linear interpolation in time between monthly mean climatological data. Wind forcing (i.e., momentum fluxes) is from *Hellerman and Rosenstein* [1983]. Surface salinities over open ocean are restored to *Levitus and Boyer* [1994] data with a time constant of 58 days. Under sea ice, fluxes of fresh water are calculated by the sea ice model, and no restoring is used. Sensible, latent, longwave, and shortwave components of the surface heat flux are calculated independently using climatological atmospheric data, calculated sea surface temperatures (SSTs), and bulk parameterizations. The data and algorithms used in the heat flux calculations are described by *Oberhuber* [1993]. No restoring of SSTs to prescribed values is used. As in many climate models, we generally Fourier filter the solution at high latitudes (poleward of  $60^\circ$ ) to eliminate high spatial frequency modes. This allows us to use longer time steps than would otherwise be numerically stable.

[8] One difficulty in performing ocean-model resolution studies involves determining values of coefficients of sub-grid-scale mixing of tracers and momentum. Since the tracer mixing terms in principle represent effects of unresolved motions upon the larger-scale (resolved) motions, the tracer mixing coefficients should be smaller with finer meshes. However, exactly how the mixing coefficients should vary with mesh size is not widely agreed upon. The philosophy we have adopted is based on an argument made by *McWilliams* [1996, 1998]. Since mesoscale eddies contain the bulk of the ocean’s kinetic energy, a simple and reasonable approach is to use the same tracer mixing coefficients at all non-eddy-resolving resolutions. According to this approach one would need to reduce tracer-mixing coefficients significantly only when the mesh becomes fine enough to start resolving mesoscale eddies. Since none of our simulations is eddy resolving, we use the same tracer-mixing coefficients in all of them. The situation

**Table 2.** Values and Rates of Change of Global Mean Potential Temperature and Salinity in Observations and in the Simulations Discussed Here

	Temperature $T$	$dT/dt$ , $\text{K (100 yr)}^{-1}$	Salinity $S$	$dS/dt$ , $\text{psu (100 yr)}^{-1}$
Observed	3.83	—	34.72	—
1 $\times$ 1	4.079	0.0063	34.775	0.00073
4 $\times$ 2 HV	4.419	0.0032	34.765	0.00027
4 $\times$ 2 LV	4.700	0.0248	34.764	0.0024

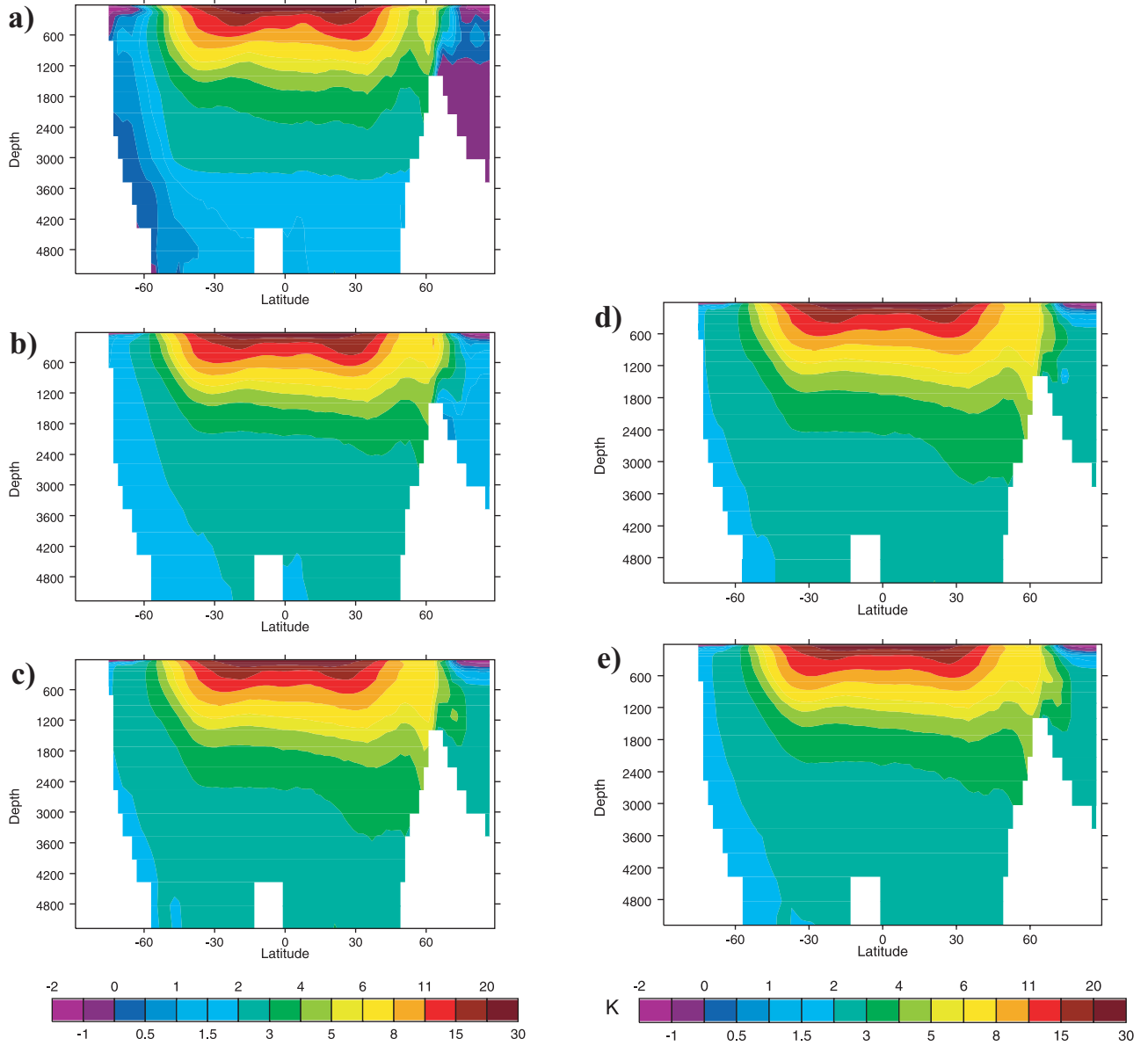


**Figure 1.** Latitude-depth sections of zonal mean potential temperature from (a) the *Levitus and Boyer* [1994] climatology, (b) the  $1 \times 1$  simulation, (c) the  $4 \times 2$  LV simulation, (d) the  $4 \times 2$  NF simulation, and (e) the  $4 \times 2$  LV simulation. Zonal means are over the full extent of the ocean. The  $1 \times 1$  data shown here have been regridded to the  $4 \times 2$  mesh.

for momentum-mixing coefficients is different than for tracer-mixing coefficients. The values of momentum-mixing coefficients (viscosities) used in typical climate simulations are much larger than is physically justifiable; these unphysically large values are required to minimize effects of numerical problems. This being the case, a defensible philosophy [McWilliams, 1996, 1998] is to use the smallest values that produce a solution that is stable and relatively free of numerically induced noise.

[9] Following this philosophy, we performed four simulations: three with a horizontal mesh of  $4^\circ$  (longitude)  $\times$   $2^\circ$  (latitude) and one with a  $1^\circ \times 1^\circ$  mesh. Distinguishing features of our four simulations are listed in Table 1. All four simulations use the same 23 levels in the vertical. Isopycnal and thickness diffusivities are the same in all four simulations (Table 1). In all simulations the slope of the

tracer-mixing surface is limited to a maximum value of 0.01. All simulations use a latitude-dependent horizontal viscosity that decreases symmetrically from the equator toward the poles, according to

$$\nu = V \left\{ 1 + 6 \exp \left[ -(\varphi/30)^2 \right] \right\}, \quad (1)$$

where  $\nu$  is horizontal viscosity,  $V$  is a scalar coefficient (values listed in Table 1), and  $\varphi$  is latitude in degrees. The higher horizontal viscosities near the equator minimize the occurrence of vertical Peclet-type instabilities near the equator [Weaver and Sarachik, 1991] by reducing vertical velocities (since these are calculated via a continuity equation). Our baseline  $4^\circ \times 2^\circ$  simulation (which we designate as  $4 \times 2$  HV, for high viscosity, uses a viscosity

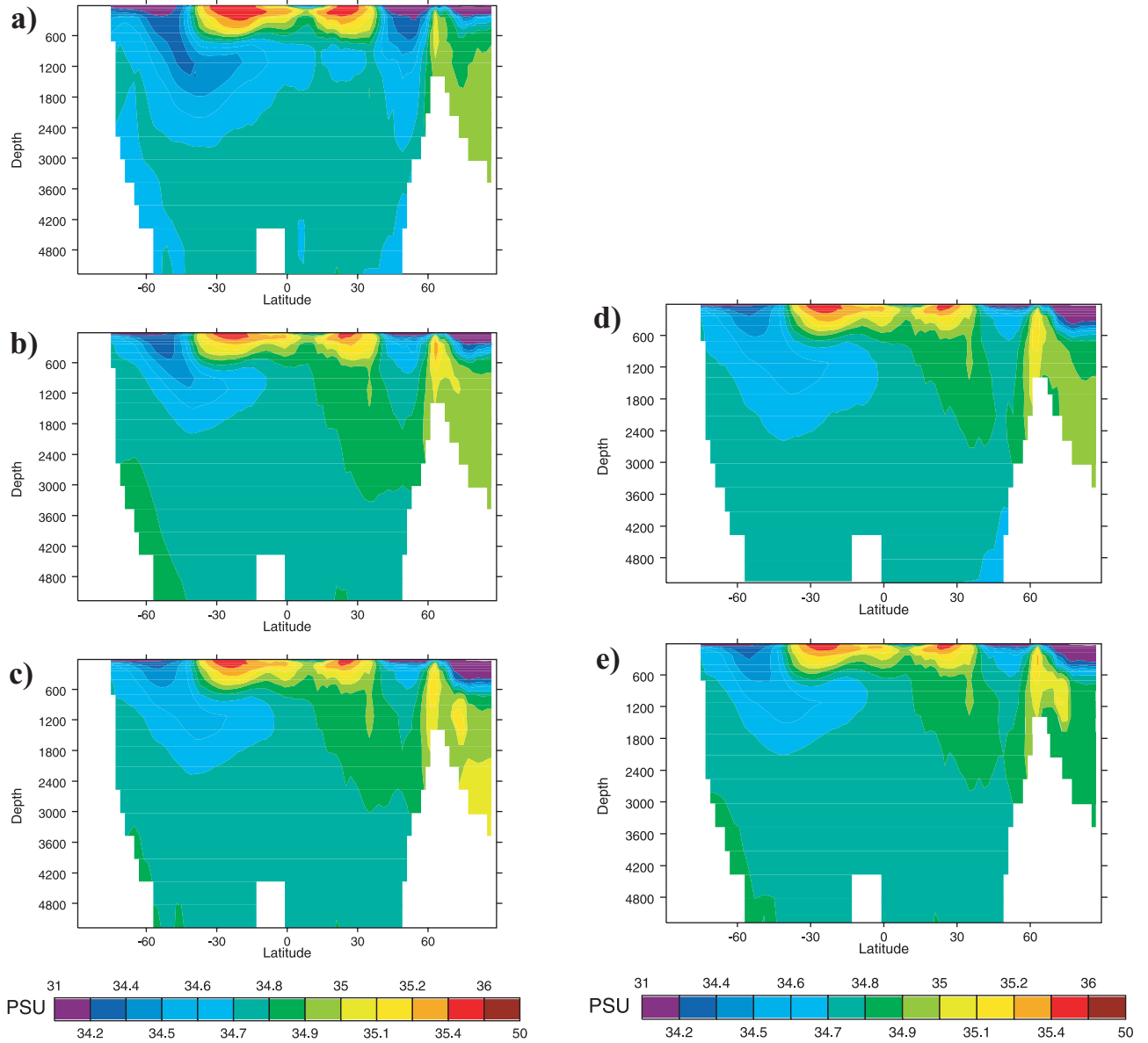


**Figure 2.** Same as Figure 1, except showing salinity.

coefficient  $V = 10^9 \text{ cm}^2 \text{ s}^{-1}$ ; this is the value we usually use at this resolution. In the  $1^\circ \times 1^\circ$  simulation we used a viscosity coefficient of  $V = 10^8 \text{ cm}^2 \text{ s}^{-1}$ , which produces viscosities that are everywhere 10 times less than those in the  $4^\circ \times 2^\circ$  HV simulation. We did this in part because using higher viscosities (to match the  $4^\circ \times 2^\circ$  HV simulation) would have required the use of a prohibitively small time step; also (as discussed above), the lower viscosities we did use are already unphysically large. This produces the unsatisfactory situation of having two simulations that differ in both grid resolution and viscosities; attributing differences in the solutions to differences in resolution or differences in viscosities would be difficult without further information. To solve this problem, we performed a second simulation at  $4^\circ \times 2^\circ$  resolution, which uses viscosities identical to the  $1^\circ \times 1^\circ$  simulation. This  $4^\circ \times 2^\circ$  LV (for low viscosity) simulation is identical to the  $1^\circ \times 1^\circ$  simulation except for horizontal grid resolution. By comparing the  $1^\circ \times 1^\circ$  results to

the  $4^\circ \times 2^\circ$  LV results we can identify effects of changing the horizontal mesh; by comparing the  $4^\circ \times 2^\circ$  LV results to the  $4^\circ \times 2^\circ$  HV results we can identify effects of changing viscosities. While it is possible to run the  $4^\circ \times 2^\circ$  code version with the lower viscosities, this is not a satisfactory default modus operandi since, as discussed above, numerical problems are apparent unless higher viscosities are used. For reasons discussed below we also performed a third  $4^\circ \times 2^\circ$  simulation; this  $4^\circ \times 2^\circ$  NF (for no filtering) simulation is identical to the  $4^\circ \times 2^\circ$  LV simulation except that no high-latitude filtering of the solution is performed.

[10] In all simulations, coefficients of vertical viscosity and diffusivity were prescribed. The coefficient of vertical viscosity is  $20 \text{ cm}^2 \text{ s}^{-1}$  everywhere. Vertical diffusivities vary from  $0.2 \text{ cm}^2 \text{ s}^{-1}$  at the surface to  $10.0 \text{ cm}^2 \text{ s}^{-1}$  at the ocean bottom.

[11] All simulations were initialized from climatological temperature and salinity values [Levitus and Boyer, 1994]

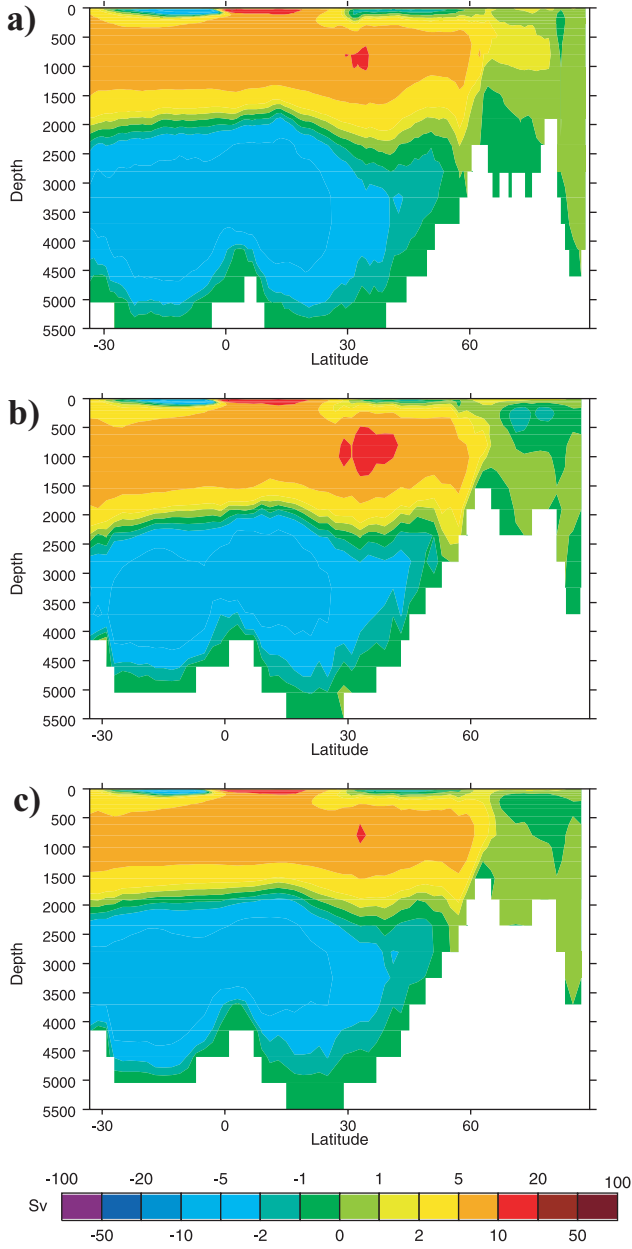


**Figure 3.** Overturning stream function in the Atlantic Ocean in (a) the  $1 \times 1$  simulation, (b) the  $4 \times 2$  LV simulation, and (c) the  $4 \times 2$  HV simulation.

with zero initial velocities. To speed the solutions' approach to equilibria, two acceleration techniques (discussed by Bryan [1984]) were used in all simulations. First, the tracer time step was longer than the momentum time steps. This “time step-splitting” accelerates the adjustment of the simulated temperature and salinity fields. Second, longer tracer time steps were used in the deep ocean compared to the surface ocean. This “deep-ocean acceleration” speeds up the adjustment of the deep-ocean solution, which otherwise would require many thousands of simulated years to reach near-equilibrium because of long ocean ventilation timescales. All simulations were run for 1500 surface years (equivalent to 11,250 years in the deepest model level) using these acceleration techniques. Then, following Dana-

basoglu *et al.* [1996], all simulations were run for 30 years with no deep-ocean acceleration. The results discussed below are averages from the last 10 years of this period. Table 2 lists global mean potential temperatures and salinities and their rates of change during this 10 year period.

### 3. Results

#### 3.1. Potential Temperature and Salinity

[12] To compare potential temperatures (hereinafter referred to as “temperatures” for simplicity) and salinities from the different simulations, we first regridded the  $1 \times 1$  result to the  $4 \times 2$  mesh. Since the  $1 \times 1$  grid is exactly commensurate with the  $4 \times 2$  mesh, this process involved averaging results from eight  $1 \times 1$  grid cells but did not

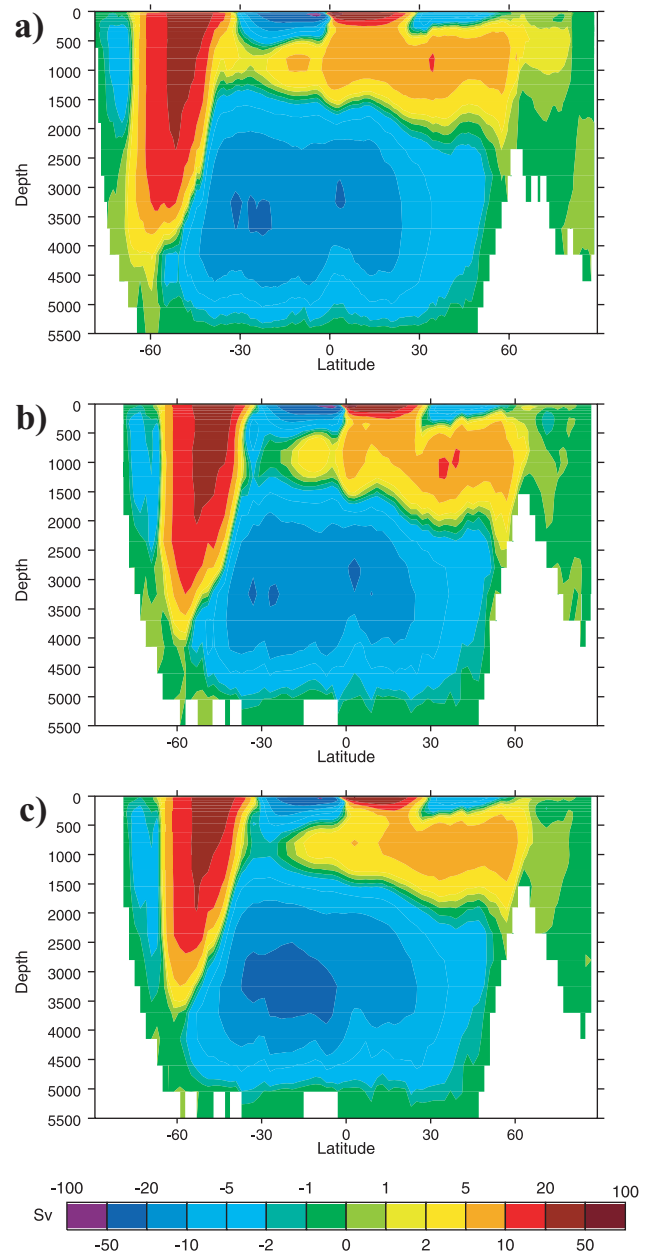


**Figure 4.** Same as Figure 3, except showing global overturning stream function.

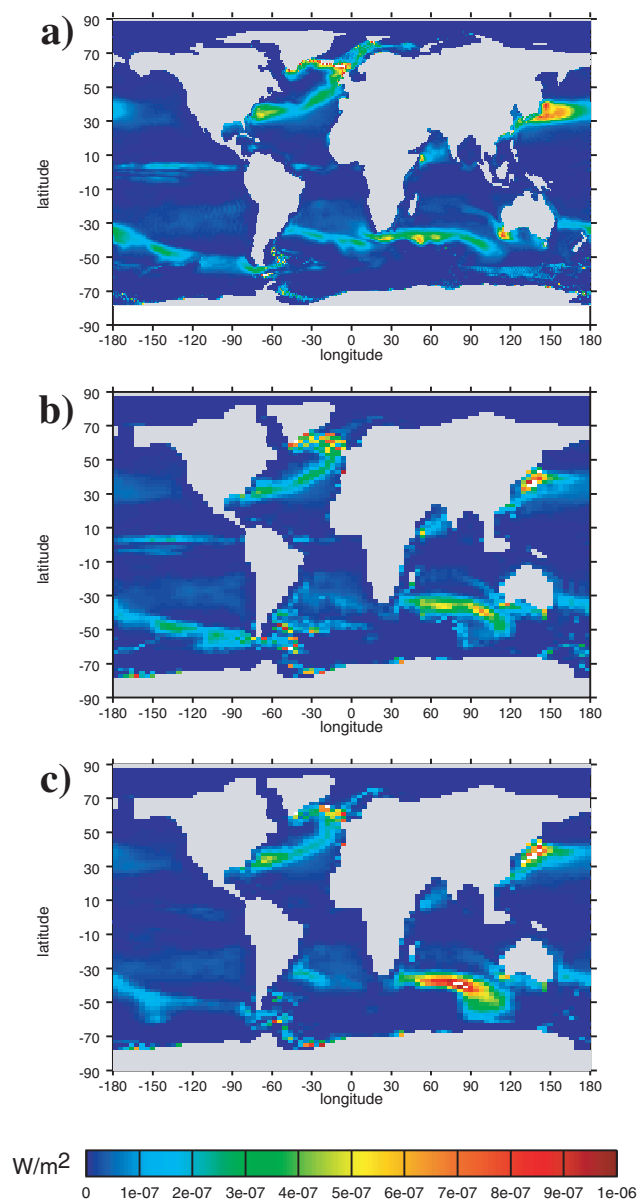


**Figure 5.** Convective activity, as measured by rate of loss of potential energy, in (a) the  $1 \times 1$  simulation, (b) the  $4 \times 2$  LV simulation, and (c) the  $4 \times 2$  HV simulation.

involve interpolation. We included in this analysis only grid cells where the  $4 \times 2$  grid cell and all eight  $1 \times 1$  cells contained therein are water cells.

[13] Latitude-depth sections of zonally averaged temperature (Figure 1) reveal a number of problems common to all the simulations. The simulated deep ocean is too warm, especially at extreme high latitudes. Although this problem is present in all the simulations, it is less severe in the  $1 \times 1$  simulation than in any of the  $4 \times 2$  simulations and less severe in the  $4 \times 2$  HV simulation than in  $4 \times 2$  LV. The problem is due in part to the absence of bottom boundary flows in our simulations; these flows bring very cold water (as well as other tracers) into the deep ocean, especially from Antarctic shelf regions. The absence of these flows in our model has been documented in previous simulations

[Caldeira and Duffy, 1998], which show that our model does not reproduce elevated concentrations of CFCs observed near the ocean floor; these elevated concentrations are thought to be produced by bottom boundary flows.

[14] The thermocline is too diffuse in all the simulations. Again, this problem is less severe in the  $1 \times 1$  simulation than in any of the  $4 \times 2$  simulations and less severe in the  $4 \times 2$  HV simulation than in  $4 \times 2$  LV. Since explicit vertical diffusivities are the same in all our simulations and since convection is typically inactive at low-latitudes and mid latitudes, one might suspect that the differences in thermocline depth between our different simulations would be due to differences in vertical advective velocities. However, this

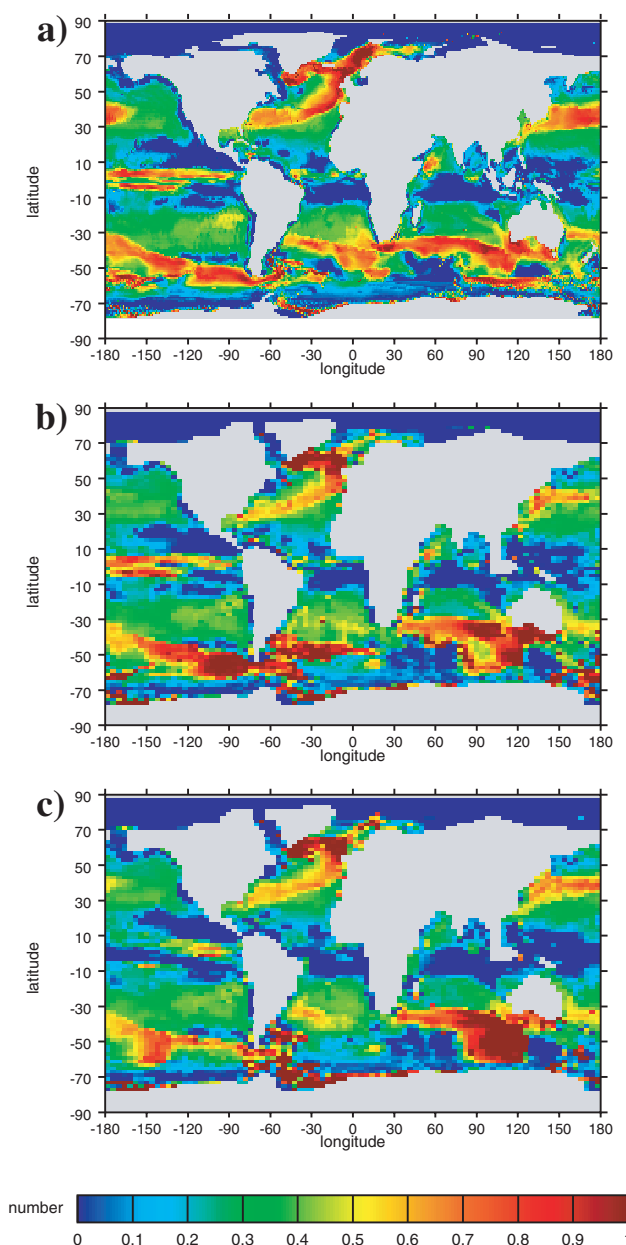


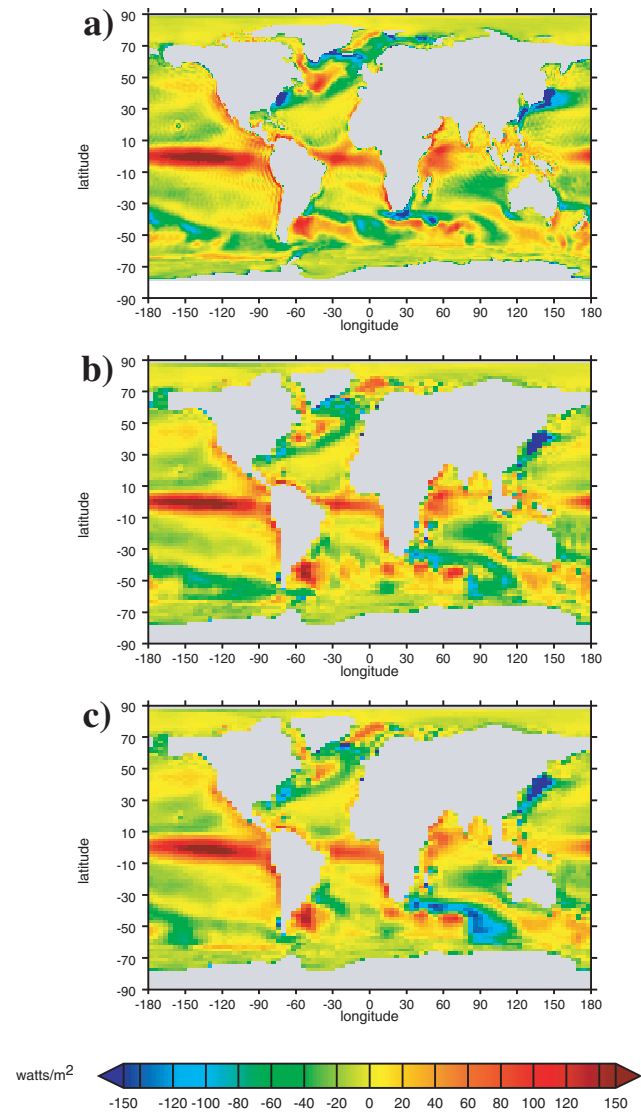
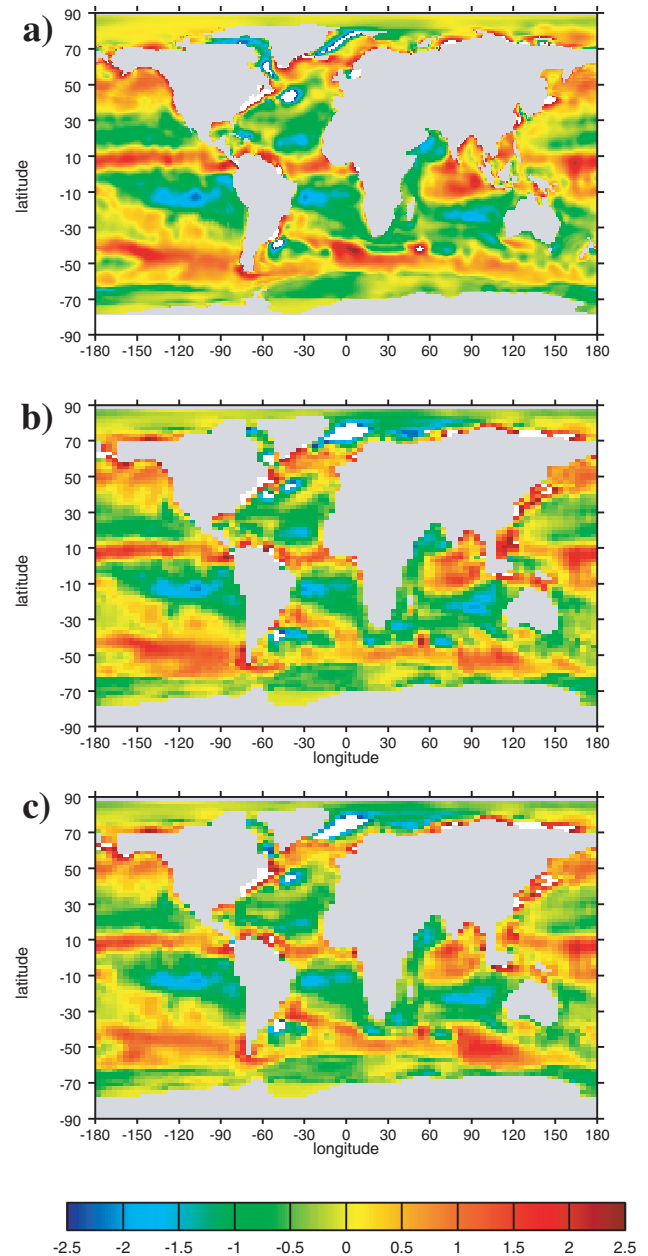
**Figure 6.** Convective activity, as measured by the fraction of time steps during which convection occurs in each vertical column in (a) the  $1 \times 1$  simulation, (b) the  $4 \times 2$  LV simulation, and (c) the  $4 \times 2$  HV simulation.

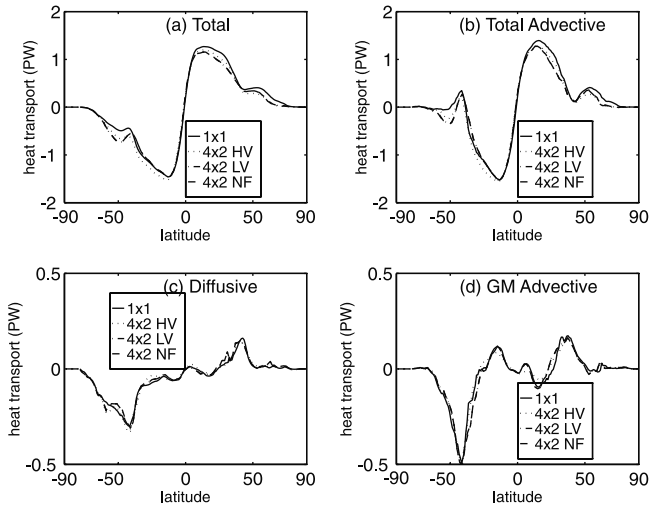
**Table 3.** Flows (in Sverdrups) Through Important Straits, As Simulated by Several Configurations of Our Model and (Where Available) As Estimated From Observations

Strait	$1 \times 1$	$4 \times 2$ LV	$4 \times 2$ HV	Observed	Observed Reference
ACC Drake Passage	136.95	137.21	115.39	118–146	Whitworth [1983]
ACC South of Africa	138.06	139.07	116.90		
ACC South of Australia	154.07	158.78	139.17		
Bering Strait	0.95	1.64	1.26	0.83±0.25	Roach <i>et al.</i> [1995]
Indonesian Throughflow	15.93	19.74	22.20		

does not seem to be the case. As expected, vertical velocities in the thermocline (not shown) are significantly smaller in the  $4 \times 2$  HV simulation than in the  $4 \times 2$  LV simulation. This occurs because larger horizontal viscosity reduced divergences of horizontal velocity, which reduces vertical velocities. This seems consistent with the fact that the thermocline is more diffuse in the  $4 \times 2$  LV simulation than in the  $4 \times 2$  HV simulation. However, vertical velocities in the  $1 \times 1$  simulation are generally as high or higher than those in the  $4 \times 2$  LV simulation, yet the

thermocline in this simulation is much “tighter” than in the  $4 \times 2$  LV simulation. Thus differences in thermocline depth between our different simulations are not due primarily to differences in vertical velocities. Rather, the main cause


**Figure 7.** Annual mean surface fluxes of heat ( $\text{W m}^{-2}$ ) in (a) the  $1 \times 1$ , (b)  $4 \times 2$  HV, and (c)  $4 \times 2$  LV simulations.

**Figure 8.** Annual mean surface fluxes of fresh water ( $\text{m yr}^{-1}$ ) in (a) the  $1 \times 1$ , (b)  $4 \times 2$  LV, and (c)  $4 \times 2$  HV simulations. The model actually uses salt fluxes; these have been converted to effective fluxes of fresh water.



**Figure 9.** Oceanic northward transport of heat in the simulations discussed here. Components shown are (a) total heat transport, (b) heat transport by advection (including the Gent-McWilliams “bolus velocity,” (c) heat transport by diffusion, and (d) heat transported by the Gent-McWilliams bolus velocity.

seems to be differences in subsurface temperatures at extreme high latitudes. For example, in the  $1 \times 1$  simulations the high-latitude, subsurface oceans are significantly colder than in the  $4 \times 2$  HV simulation, whose subsurface oceans in turn are colder than in the  $4 \times 2$  LV simulation. Lateral mixing between high latitudes and lower latitudes means this colder high-latitude water tends to have a cooling effect on the thermocline region. Thus the thermocline is shallower in the  $1 \times 1$  simulation than in the  $4 \times 2$  HV simulation, which in turn is shallower than the thermocline in the  $4 \times 2$  LV simulation.

[15] Latitude-depth sections of zonally averaged salinity (Figure 2) show strong similarities between all our simulations. The most noticeable differences are in the Arctic, where the  $1 \times 1$  simulation agrees better with observations than the  $4 \times 2$  HV or  $4 \times 2$  LV simulation. The deep Southern Ocean is too salty in all our simulations, but this problem is slightly worse in the  $1 \times 1$  simulation than in the  $4 \times 2$  HV or  $4 \times 2$  LV simulation.

[16] The relatively large differences in simulated temperatures and salinities in the Arctic between the  $1 \times 1$  and  $4 \times 2$  simulations suggested an interesting experiment. If, as our results suggest, higher horizontal resolution is especially helpful at extreme high latitudes, then it might be useful to

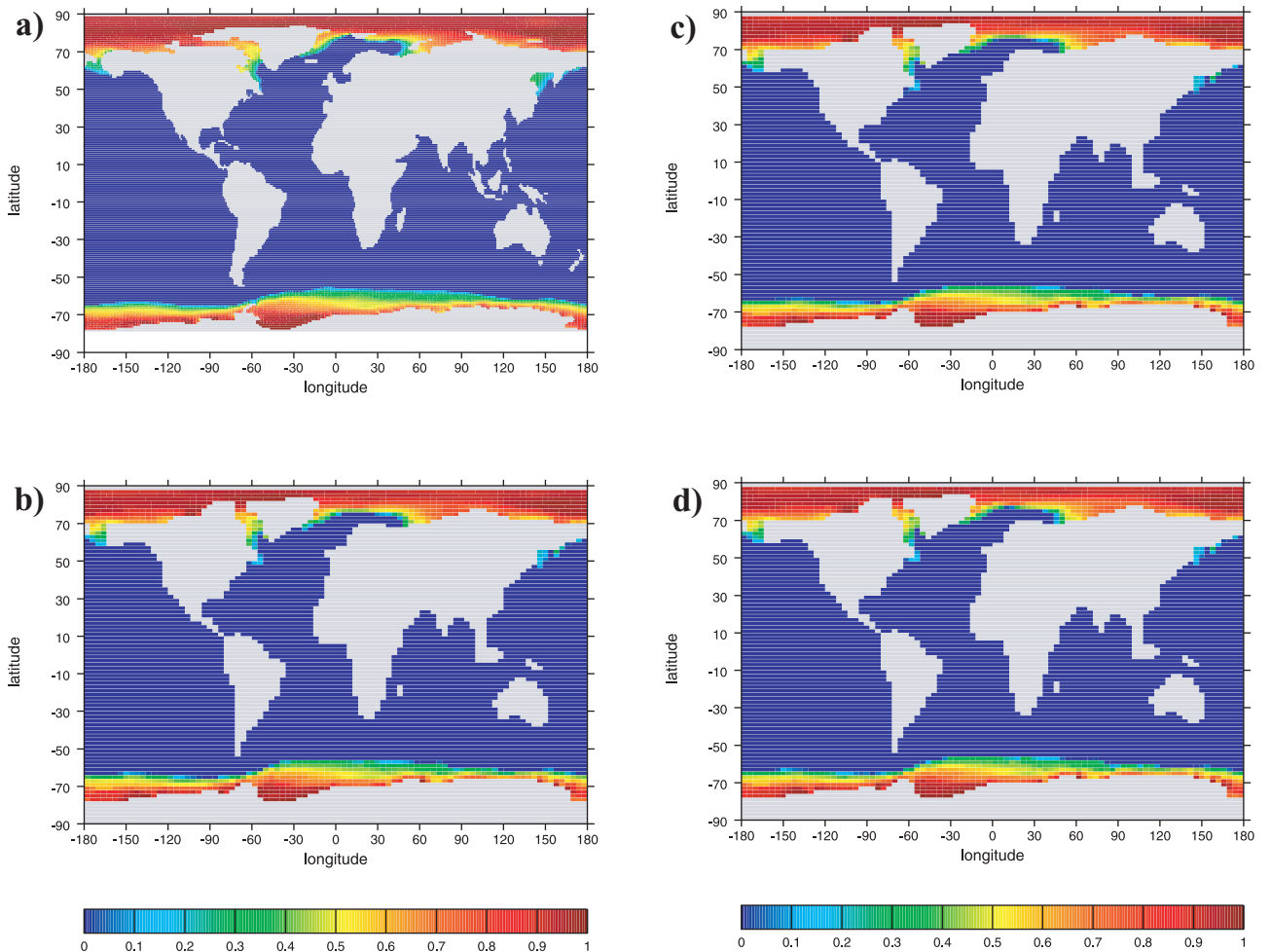


**Figure 10.** Sea ice concentration (fraction of area covered by ice) in the (a)  $1 \times 1$ , (b)  $4 \times 2$  LV, (c)  $4 \times 2$  HV, and (d)  $4 \times 2$  NF simulations. Results shown are annual means.

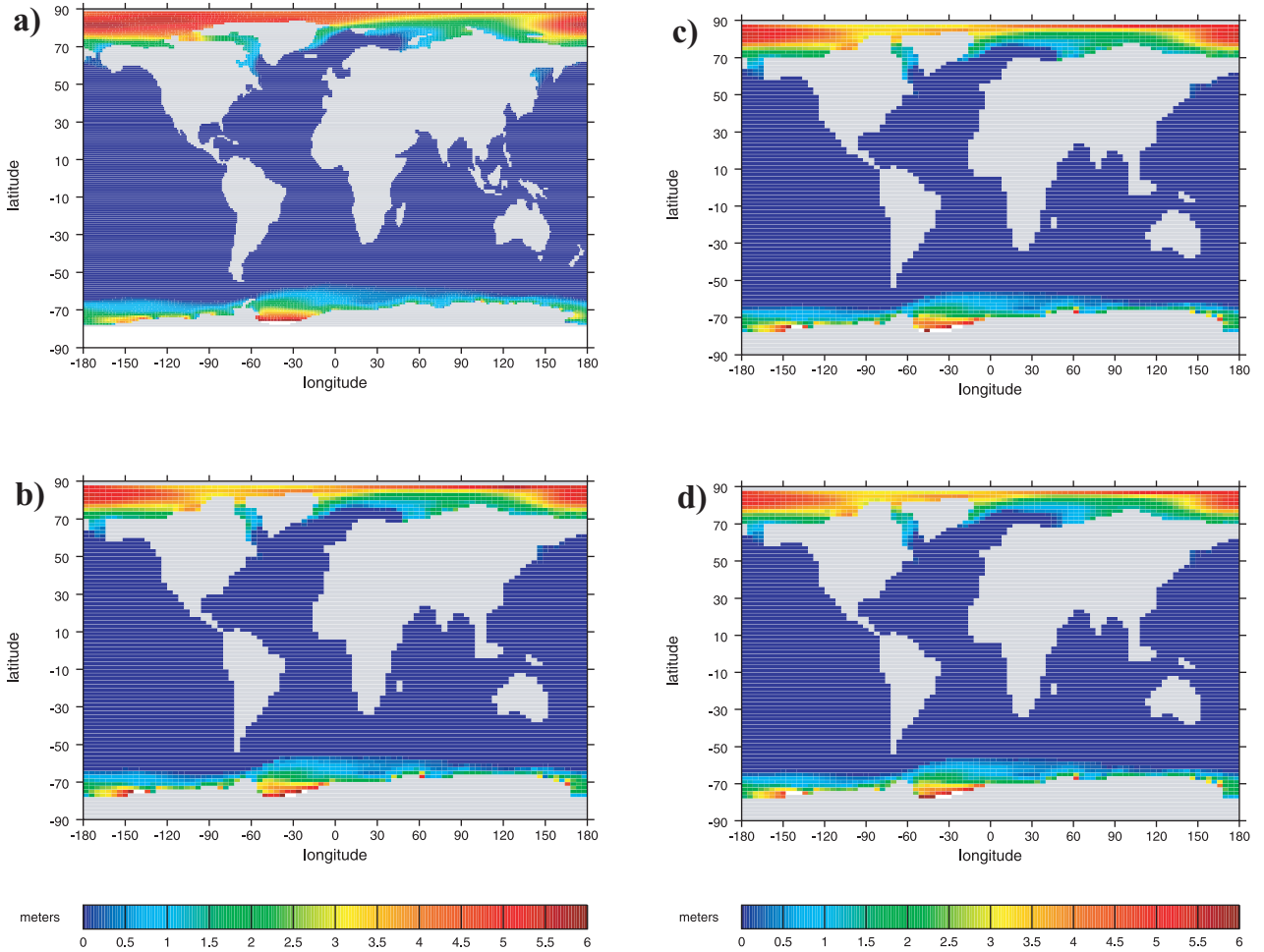


**Figure 11.** Annual mean sea ice thickness in the (a)  $1 \times 1$ , (b)  $4 \times 2$  LV, (c)  $4 \times 2$  HV, and (d)  $4 \times 2$  NF simulations.

run the model at coarse resolution without high-latitude filtering. The rationale for this is that latitude-longitude coordinates on a sphere automatically produce high resolution in the zonal direction at high latitudes. Our normal modus operandi, however, is to effectively coarsen the resolution at high latitudes by filtering the solution in these regions. Thus eliminating high-latitude filtering might provide much of the benefit of going to higher horizontal resolution (since this seems to be where the biggest differences between the  $1 \times 1$  and  $4 \times 2$  simulations occur). If the computational cost of running without filtering is less than that of running at high resolution everywhere, then running at coarse resolution without filtering might be a more cost-effective improvement over the standard  $4 \times 2$  configuration than running with filtering at either coarse or fine resolution.

[17] To test this hypothesis, we performed another simulation at  $4 \times 2$  resolution that is similar to the  $4 \times 2$  LV simulation, except that no high-latitude filtering is used. We call this the  $4 \times 2$  NF simulation (Table 1). In order to maintain numerical stability we had to reduce the time steps in this simulation by a factor of 6 compared to those used in the other  $4 \times 2$  simulations. (The only differences between the  $4 \times 2$  LV and  $4 \times 2$  NF simulations are the time steps and the presence or absence of filtering.) Thus the  $4 \times 2$  NF

simulation is 6 times as expensive computationally as the other  $4 \times 2$  simulations. This is still significantly cheaper than the  $1 \times 1$  simulation, which is 32 times as expensive as either the  $4 \times 2$  LV or the  $4 \times 2$  HV simulations. (A factor of 8 comes from the increase in the number of grid cells; the additional factor of 4 results from the shorter time step needed to maintain numerical stability.)

[18] Zonally averaged temperatures (Figure 1) are very similar in the  $4 \times 2$  LV and  $4 \times 2$  NF simulations. Thus eliminating high-latitude filtering seems to have little effect on this aspect of the solution. Zonally averaged salinities, however, are distinctly different in the  $4 \times 2$  NF simulation from those in the  $4 \times 2$  LV simulation (Figure 2). In the Arctic Ocean, salinities in the  $4 \times 2$  NF simulation agree more closely with those in both the Levitus climatology and the  $1 \times 1$  simulation than do Arctic salinities in the  $4 \times 2$  LV simulation. Thus, as far as Arctic salinities are concerned, eliminating high-latitude filtering appears to produce nearly as much improvement in the solution as going to  $1 \times 1$  resolution, at much less computational expense.

### 3.2. Meridional Overturning, Convection, and Flow Through Straits

[19] The meridional overturning stream function appears very similar in all our simulations (Figures 3 and 4). In the

Atlantic sector the maximum strength of overturning is between 10 and 11 Sv in the  $1 \times 1$  and  $4 \times 2$  HV simulations and between 12 and 13 Sv in the  $4 \times 2$  LV simulation. The maximum depth of penetration of North Atlantic Deep Water is very similar in all the simulations (between 2000 and 2500 m).

[20] Significant differences between our three simulations are evident in two different measures of convective activity (Figures 5 and 6). The first of these is the vertically integrated rate of loss of potential energy due to convection. This measures buoyancy transported by convection. The second measure of convective activity is related to how often convection occurs; it is the fraction of time steps during which convection occurs anywhere in each vertical column. For both measures of convective activity, areas of strong convection tend to be smaller in the  $1 \times 1$  simulation than in either of the  $4 \times 2$  simulations; this is especially true in the Southern Ocean.

[21] Table 3 lists flows through several straits in our simulations. In the Antarctic Circumpolar Current (ACC), the flows are much more sensitive to the viscosity difference between our two  $4 \times 2$  simulations than to the difference in resolution between the  $4 \times 2$  and  $1 \times 1$  simulations. As expected, the ACC is more sluggish at the higher viscosity. The higher flow through the Bering Strait in the  $4 \times 2$  simulations occurs because the strait is much wider in these simulations than in the  $1 \times 1$  simulation. At both resolutions the Bering Strait is three tracer grid cells wide; with the staggered computational mesh this allows advective flows at two velocity points. Thus, in the  $4 \times 2$  simulations the Bering Strait is  $12^\circ$  of longitude wide versus only  $3^\circ$  in the  $1 \times 1$  simulation. Similarly, flow between Indonesia and Australia goes through a narrower strait in the  $1 \times 1$  simulation ( $11^\circ$  in the N-S direction) than in the  $4 \times 2$  simulations ( $16^\circ$  in the N-S direction).

[22] The relatively weak sensitivity of meridional overturning and flows through straits in our simulations to model resolution contrasts sharply with the results of *Washington et al.* [1994]. They find (for example) that the simulated flow through the Drake Passage is 6 times stronger at  $1^\circ$  resolution than at  $5^\circ$  resolution. We can only speculate that the large differences they found result from the very different vertical resolutions used in their different runs and from examining the model solution before it has reached near-equilibrium.

### 3.3. Surface Fluxes and Latitudinal Heat Transport

[23] Since the surface fluxes of heat and fresh water are formulated identically in all our simulations, differences in these fluxes between the different simulations will reflect differences in surface ocean properties. In particular, both heat and freshwater fluxes are sensitive to simulated SSTs. Since convection is the most rapid mechanism for vertical transport of heat and salinity, it is not surprising that the largest differences in surface fluxes between the different simulations (Figures 7 and 8) occur in the same locations as the largest differences in rates of convective activity.

[24] Despite these differences the surface fluxes of heat and fresh water are on the whole very similar in our simulations. This contrasts sharply with the results of *Washington et al.* [1994] who found first-order differences in surface fluxes

between simulations performed at  $5^\circ$ ,  $1^\circ$ , and  $0.5^\circ$  resolutions. The large differences found by *Washington et al.* may have resulted from the much coarser vertical resolution (four levels in the vertical) used in the  $5^\circ$  than in the finer-resolution simulations (which used 20 levels in the vertical). Another factor may be the relatively short model runs (100 years) that they performed. If the surface fluxes were examined while the model solution was rapidly adjusting, the fluxes could be very different from their near-equilibrium values.

[25] The latitudinal transport of heat by the ocean is comparable to that of the atmosphere and plays an important role in determining Earth's climate. Thus realistic simulation of oceanic latitudinal heat transport, both in present and future climates, is important. The differences in total northward heat transport between our various simulations (Figure 9) are small compared to the difference between any of the simulations and observation-based estimates [e.g., *Trenberth and Solomon*, 1994]. For example, observation-based estimates have a maximum Northern Hemisphere heat transport in excess of 2 PW, whereas the Northern Hemisphere maxima in all our simulations are between 1.1 and 1.3 PW. It may be significant, however, that of all our simulations the  $1 \times 1$  is closest to the observation-based estimate of maximum heat transport in the Northern Hemisphere. Figure 9 also shows that the differences between different simulations are small for the different components (advective, diffusive, etc.) of latitudinal heat transport.

[26] Our results contrast those of *Fanning and Weaver* [1997], who found that latitudinal heat transport in the ocean component of their idealized coupled model has a significant resolution dependence. A possible reason why their results differ from ours is that their finer-resolution simulations were run for much shorter times than their coarse-resolution simulations; this was presumably a computational necessity. Thus their coarse-resolution simulations were no doubt much closer to equilibrium. It is also possible that the use of horizontal Laplacian mixing by *Fanning and Weaver* (as opposed to our use of the Gent-McWilliams eddy parameterization) results in a stronger dependence of latitudinal heat transport on resolution. Finally, the presence of an interactive (albeit simplified) atmospheric model in the *Fanning and Weaver* simulations may produce increased sensitivity to ocean model resolution compared to simulations like ours that are constrained by the upper boundary conditions.

### 3.4. Sea Ice

[27] In our model the ocean and sea ice components use the same horizontal computational mesh. Because ice velocities are lower than those of the ocean, no high-latitude filtering of sea ice variables is needed or performed. Figures 10 and 11 show that annual mean sea ice thicknesses and compactnesses are remarkably similar in all our simulations. The most significant difference between any of our simulations seems to be that sea ice thicknesses in the Arctic are slightly greater in the  $1 \times 1$  simulation than in the others. Observations of ice thickness are not comprehensive enough to allow us to tell which simulation is more realistic in this respect. Thus we find that the ice model results are not highly sensitive to the horizontal grid, the horizontal

ocean viscosity, or the presence or absence of high-latitude filtering of ocean variables.

#### 4. Conclusions

[28] This study examines the effect of horizontal grid resolution on the near-equilibrium solution of a global ocean-sea ice model. We compare one simulation using a  $1^\circ \times 1^\circ$  horizontal mesh to three simulations that use a  $4^\circ$  (longitude)  $\times$   $2^\circ$  (latitude) horizontal mesh. Our comparison emphasizes large-scale aspects of the solution relevant to climate simulation. Since none of our simulations resolves mesoscale eddies, our results do not assess the possible importance of resolving eddies in climate simulations. In addition, we have looked only at time-averaged solutions; thus our results do not assess possible sensitivity of simulated time variability to horizontal resolution. Finally, in our study the solutions are strongly constrained by surface boundary conditions; a coupled ocean-atmosphere model might display stronger sensitivity to ocean model resolution. There are significant differences between the  $1 \times 1$  and  $4 \times 2$  solutions, and in general, the  $1 \times 1$  results are closer to observations than the  $4 \times 2$  results are. In particular, the following aspects of the  $1 \times 1$  simulation are more realistic: temperatures and salinities in the Arctic Ocean, temperatures in the deep Southern Ocean, vertical temperature gradients in the thermocline, and latitudinal heat transport. Nonetheless, the differences between the  $1 \times 1$  and  $4 \times 2$  results are always much smaller than the differences between any simulation and available observations. Thus our results show that the near-equilibrium mean solution of our model is not highly sensitive to resolution for simulations outside the eddy-resolving regime. These results therefore suggest that the best approach to improving the results of coarse-resolution ocean models is not modest increases in resolution outside the eddy-resolving regime but rather other approaches such as improved numerical methods, better parameterizations of sub-grid-scale processes, or better forcing data.

#### References

- Bryan, K., Accelerating the convergence to equilibrium of ocean climate models, *J. Phys. Oceanogr.*, **14**, 666–673, 1984.
- Bryan, F. O., and R. D. Smith, Modeling the North Atlantic circulation: From eddy-resolving to eddy-permitting, *Int. WOCE Newsl.*, **33**, 12–14, 1998.
- Caldeira, K., and P. B. Duffy, Sensitivity of simulated CFC-11 distributions in a global ocean model to the treatment of salt rejected during sea-ice formation, *Geophys. Res. Lett.*, **25**, 1003–1006, 1998.
- Covey, C., Global ocean circulation and equator-pole heat transport as a function of ocean GCM resolution, *Clim. Dyn.*, **11**, 425–437, 1995.
- Danabasoglu, G., J. C. McWilliams, and W. G. Large, Approach to Equilibrium in accelerated global oceanic models, *J. Clim.*, **9**, 1092–1110, 1996.
- Duffy, P. B., and K. Caldeira, Sensitivity to simulated salinity in a three-dimensional ocean model to upper-ocean transport of salt from sea-ice formation, *Geophys. Res. Lett.*, **24**, 1323–1326, 1997.
- Fanning, A. F., and A. J. Weaver, A horizontal resolution and parameter sensitivity study of heat transport in an idealized coupled climate model, *J. Clim.*, **10**, 2469–2478, 1997.
- Gent, P. R., and J. C. McWilliams, Isopycnal mixing in ocean general circulation models, *J. Phys. Oceanogr.*, **20**, 150–155, 1990.
- Gent, P. R., F. Bryan, G. Danabasoglu, S. Doney, W. Holland, W. Large, and J. McWilliams, The NCAR Climate System Model ocean component, *J. Clim.*, **11**, 1287–1306, 1998.
- Hellerman, S., and M. Rosenstein, Normal monthly wind stress over the world ocean with error estimates, *J. Phys. Oceanogr.*, **13**, 1093–1104, 1983.
- Killworth, P. D., D. Stainforth, D. J. Webb, and S. M. Paterson, The development of a free-surface Bryan-Cox-Semtner ocean model, *J. Phys. Oceanogr.*, **21**, 1333–1348, 1991.
- Levitus, S., and T. P. Boyer, *World Ocean Atlas 1994*, vol. 4, *Temperature*, NOAA Atlas NESDIS, vol. 4, 129 pp., Natl. Ocean. and Atmos. Admin., Silver Spring, Md., 1994.
- McAvaney, B., et al., Model evaluation, in *IPCC Third Assessment Report*, Intergov. Panel on Clim. Change, Geneva, 2001.
- McClean, J., A. J. Semtner, and V. Zlotnicki, Comparisons of mesoscale variability in the Semtner-Chervin  $1/4^\circ$  model, the Los Alamos Parallel Ocean Program  $1/6^\circ$  model, and TOPEX/Posidon data, *J. Geophys. Res.*, **102**, 25,203–25,226, 1997.
- McWilliams, J. C., Modeling the oceanic general circulation, *Annu. Rev. Fluid Mech.*, **28**, 1–34, 1996.
- McWilliams, J. C., Oceanic general circulation models, in *Ocean Modeling and Parameterization*, edited by E. Chassignet, pp. 1–44, Kluwer Acad. Norwell, Mass, 1998.
- Oberhuber, J. M., Simulation of the Atlantic circulation with a coupled sea ice-mixed layer-isopycnal general circulation model, part I, Model description, *J. Phys. Oceanogr.*, **23**, 808–829, 1993.
- Roach, A. T., K. Aagard, C. H. Pease, S. A. Salo, T. Weingartner, V. Pavlov, and M. Kulakov, Direct measurement of transport and water properties through the Bering Strait, *J. Geophys. Res.*, **100**, 18,443–18,457, 1995.
- Semtner, A. J., Jr., and R. M. Chervin, A simulation of the global ocean circulation with resolved eddies, *J. Geophys. Res.*, **93**, 15,502–15,522, 1988.
- Semtner, A. J., Jr., and R. M. Chervin, Ocean general circulation from a global eddy-resolving model, *J. Geophys. Res.*, **97**, 5493–5550, 1992.
- Trenberth, K. E., and A. Solomon, The global heat balance—Heat transports in the atmosphere and ocean, *Clim. Dyn.*, **10**, 107–134, 1994.
- Washington, W. M., G. A. Meehl, L. VerPlank, and T. Bettge, A world ocean model for greenhouse sensitivity studies: Resolution intercomparison and the role of diagnostic forcing, *Clim. Dyn.*, **9**, 321–344, 1994.
- Weaver, A. J., and E. S. Sarachik, On the importance of vertical resolution in certain oceanic general circulation models—Reply, *J. Phys. Oceanogr.*, **21**, 1702–1707, 1991.
- Whitworth, T., III, Monitoring the transport of the Antarctic Circumpolar Current at Drake Passage, *J. Phys. Oceanogr.*, **13**, 2045–2057, 1983.
- Wickett, M. E., P. B. Duffy, and G. Rodrigue, A reduced grid for a parallel global ocean general circulation model, *Ocean Model.*, **2**, 85–107, 2000.

K. Caldeira and P. B. Duffy, Climate System Modeling Group, Lawrence Livermore National Laboratory, L-103, P.O. Box 808, 7000 East Avenue, Livermore, CA 94550, USA. (pduffy@llnl.gov)

M. E. Wickett, Center for Applied Scientific Computing, Lawrence Livermore National Laboratory, L-103, P.O. Box 808, 7000 East Avenue, Livermore, CA 94550, USA.